added to the exterior air film resistance of 0.03 $m^2 \cdot K/W$ and the interior air film resistance of 0.12 $m^2 \cdot K/W$ (from Table 1, Chapter 25), the total resistance is 3.65 $m^2 \cdot K/W$ and the U-factor is 1/3.65 = 0.274 $W/(m^2 \cdot K)$. The edge-of-spandrel U-factor is 40% of the way to the frame U-factor, which is 0.274 + [0.40(9.94 – 0.274)] = 4.14 $W/(m^2 \cdot K)$.

$$U_{opaque\ spandrel\ module} = \frac{(0.274 \times 0.9801) + (4.14 \times 0.2743) + (9.94 \times 0.1856)}{(1.2 \times 1.2)} = 2.26\ W/(m^2 \cdot K)$$

Finally, calculate the overall average U-factor for the curtain wall assembly, including the one module of vision glass and the two modules of opaque spandrel.

$$U_{curtain\ wall} = \frac{[3.41 \times (1.2 \times 1.2)] + [2.26 \times 2 \times (1.2 \times 1.2)]}{3 \times (1.2 \times 1.2)} = 2.64\ W/(m^2 \cdot K)$$

Note that even with double glazing having a low-e coating and with R-20 in the opaque areas, this curtain wall with metal pans only has an overall R-value of approximately 0.38 $m^2 \cdot K/W$.

Example 4. Estimate the U-factor for a semicircular barrel vault that is 6 m wide (3 m tall) and 10 m long mounted on a 150 mm curb. The barrel vault has an aluminum frame without a thermal break. The glazing is double with a 13 mm gap width filled with air and a low-e coating (e = 0.20).

Solution: An approximation can be made by multiplying the U-factor for a site-assembled sloped/overhead glazing product having the same frame and glazing features by the ratio of the surface area (including the curb) of the barrel vault to the rough opening area in the roof that the barrel vault fits over. First, determine the surface area (including the curb) of the barrel vault:

Area of the curved portion of the barrel vault
= (π × diameter/2) × length
= (3.14 × 6/2) × 10 = 94.25 m^2

Area of the two ends of the barrel vault
= $2\pi(\text{radius}^2)/2 = \pi r^2$
= 3.14 × 32 = 28.27 m^2

Area of the curb
= perimeter × curb height
= (6 + 10 + 6 + 10) × 0.150 = 4.8 m^2

Total surface area of the barrel vault
= 94.25 + 28.27 + 4.8 = 127.3 m^2

Second, determine the rough opening area in the roof that the barrel vault fits over:
= length × width
= 6 × 10 = 60 m^2

Third, determine the ratio of the surface area to the rough opening area:
= 127.3/60 = 2.12

Fourth, determine the U-factor from Table 4 of a site-assembled sloped/overhead glazing product having the same frame and glazing features. The U-factor is 4.06 $W/(m^2 \cdot K)$ (ID = 17, 12th column on the second page of Table 4).

Fifth, determine the estimated U-factor of the barrel vault.

$U_{barrel\ vault}$
= $U_{sloped\ overhead\ glazing}$ × surface area/rough opening for the barrel vault
= 4.06 × 2.12 = 8.61 $W/(m^2 \cdot K)$

SOLAR HEAT GAIN AND VISIBLE TRANSMITTANCE

Fenestration solar heat gain has two components. First is directly transmitted solar radiation. The quantity of radiation entering the fenestration directly is governed by the solar transmittance of the glazing system. Multiplying the incident irradiance by the glazing area and its solar transmittance yields the solar heat entering the fenestration directly. The second component is the absorbed solar radiation, radiation that is removed from the main beam and absorbed in the glazing and framing materials of the window, some of which is subsequently conducted to the interior of the building.

DETERMINING INCIDENT SOLAR FLUX

Solar Radiation

The flux of solar radiation on a surface normal (perpendicular) to the sun's rays above the earth's atmosphere at the mean earth-sun distance of 149.5×10^6 km (Allen 1973) is defined as the solar constant E_{sc}. The currently accepted value is 1367 W/m^2 (Iqbal 1983). Because the earth's orbit is slightly elliptical, the extraterrestrial radiant flux E_o varies from a maximum of 1413 W/m^2 on January 3, when the earth is closest to the sun (aphelion), to a minimum of 1332 W/m^2 on July 4, when the earth-sun distance reaches its maximum (perihelion).

The earth's orbital velocity also varies throughout the year, so **apparent solar time**, as determined by a solar time sundial, varies somewhat from the **mean time** kept by a clock running at a uniform rate. This variation, called the **equation of time**, is given in Table 7. The conversion between local standard time and solar time involves two steps. First the equation of time is added to the local standard time, and then a longitude correction is added. This longitude correction is four minutes of time per degree difference between the local (site) longitude and the longitude of the **local standard meridian** for that time zone. Standard meridians are found every 15° from 0° at Greenwich, England (Greenwich Meridian). In the United States and Canada, these values are 60° for Atlantic Standard Time, 75° for Eastern Standard Time, 90° for Central Standard Time, 105° for Mountain Standard Time, 120° for Pacific Standard Time, 135° for Alaska Standard Time, and 150° for Hawaii-Aleutian Standard Time.

Equation (10) relates apparent solar time (AST) to local standard time (LST) as follows:

$$\text{AST} = \text{LST} + \text{ET}/60 + (\text{LSM} - \text{LON})/15 \tag{10}$$

where

AST = apparent solar time, decimal hours
LST = local solar time, decimal hours
ET = equation of time, decimal minutes
LSM = local standard time meridian, decimal ° of arc
LON = local longitude, decimal ° of arc

Because the earth's equatorial plane is tilted at an angle of 23.45° to the orbital plane, the **solar declination** δ (the angle between the

Table 7 Extraterrestrial Solar Irradiance and Related Data

	E_o, W/m^2	Equation of Time, min	Declination, degrees	*A* W/m^2	*B* (Dimensionless Ratios)	*C* (Dimensionless Ratios)
Jan	1416	−11.2	−20.0	1230	0.142	0.058
Feb	1401	−13.9	−10.8	1215	0.144	0.060
Mar	1381	−7.5	0.0	1186	0.156	0.071
Apr	1356	1.1	11.6	1136	0.180	0.097
May	1336	3.3	20.0	1104	0.196	0.121
June	1336	−1.4	23.45	1088	0.205	0.134
July	1336	−6.2	20.6	1085	0.207	0.136
Aug	1338	−2.4	12.3	1107	0.201	0.122
Sep	1359	7.5	0.0	1151	0.177	0.092
Oct	1380	15.4	−10.5	1192	0.160	0.073
Nov	1405	13.8	−19.8	1221	0.149	0.063
Dec	1417	1.6	−23.45	1233	0.142	0.057

Note: Data are for 21st day of each month during the base year of 1964.

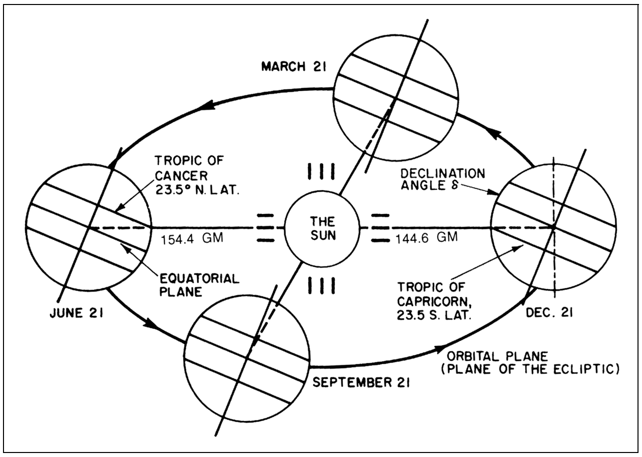

Fig. 6 Motion of Earth around Sun

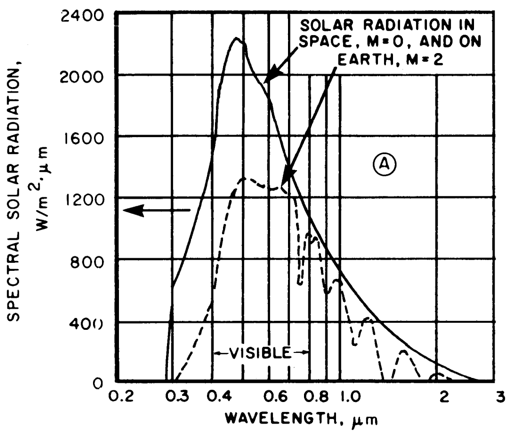

Fig. 7 Terrestrial and Extraterrestrial Solar Spectral Irradiances

earth-sun line and the equatorial plane) varies through out the year, as shown in Figure 6, Table 7, and Equation (11). This variation causes the changing seasons with their unequal periods of daylight and darkness. The following equation can be used to estimate the declination from the day of year η, but it is more accurate to look up the actual declination in an astronomical or nautical almanac for the actual year and date in question.

$$\delta = 23.45 \sin \{[360(284 + \eta)]/365\} \quad (11)$$

The spectral distribution of solar radiation beyond the earth's atmosphere (Figure 7) resembles the radiant energy emitted by a blackbody at about 6000 K. The peak solar spectral irradiance of 2130 $W/(m^2 \cdot K)$ is reached at 0.451 μm (451 nm) in the green portion of the visible spectrum.

In passing through the earth's atmosphere, the sun's radiation is reflected, scattered, and absorbed by dust, gas molecules, ozone, water vapor, and water droplets (fog and clouds). The extent of this depletion at any given time is determined by atmospheric composition and length of the atmospheric path traversed by the sun's rays. This length is expressed in terms of the air mass m, which is the ratio of the mass of atmosphere in the actual earth-sun path to the mass that would exist if the sun were directly overhead at sea level (m = 1.0). For most purposes, the air mass at any time equals the cosecant of the solar altitude multiplied by the ratio of the existing barometric pressure to standard pressure. Beyond the atmosphere, m = 0.

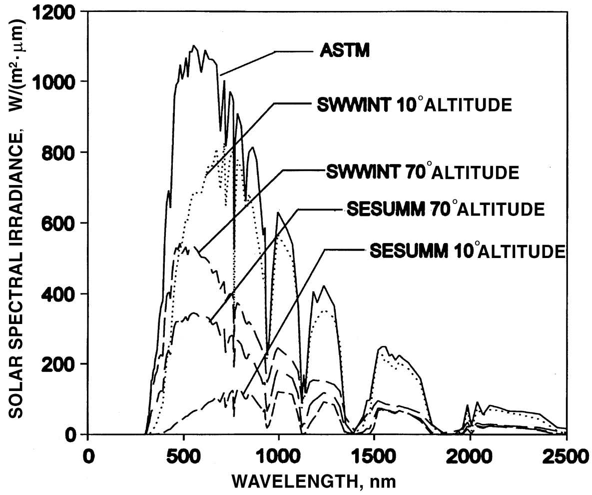

Fig. 8 Comparison of Standard Air Mass m = 1.5 Solar Spectrum with Direct Beam Spectra Through Atmospheres

Characteristic of southwest in winter (SWWINT) and southeastern U.S. in summer (SESUMM) for two solar altitude angles (McCluney 1996)

Table 8 Portions of Total Solar Spectral Irradiance Contained in Portions of Visible Spectrum

Wavelength, nm		Percent Irradiance	Percent Illuminance
Start	End		
370	770	54.4	100.0
380	760	52.2	100.0
390	750	50.2	99.9
400	740	47.4	99.9
410	730	44.9	99.8
420	720	41.9	99.8
430	710	39.5	99.8
440	700	36.7	99.8
450	690	35.3	99.5
460	680	31.1	99.1

Note: The integrated total irradiance = 950 W/m^2 and illuminance = 100 klx.

Most ultraviolet solar radiation is absorbed by the ozone in the upper atmosphere, while part of the radiation in the short-wave portion of the spectrum is scattered by air molecules, imparting the blue color to the sky. Water vapor in the lower atmosphere causes the characteristic absorption bands observed in the solar spectrum at sea level (Figure 7). For a solar altitude β of 41.8° (air mass m = 1.5), the total solar direct beam flux on a clear day at sea level can be divided into spectral regions as follows. Less than 3% of the total is in the ultraviolet, 47% is in the visible region, and the remaining 50% is in the infrared (ASTM *Standard* E 891). The maximum spectral irradiance occurs at 0.61 μm, and little solar energy (less than 5% of the spectrum) exists at wavelengths beyond 2.1 μm.

It is interesting to see what fraction of the total solar irradiance lies in the visible part of the spectrum. Since the limits of the visible portion vary from observer to observer (and because the eye is not very sensitive to radiation at the spectral limits of vision), the fractions of total irradiance and illuminance found between different spectral limits at the edge of the visible portion of the spectrum can be calculated. The results are shown in Table 8 for the ASTM air mass m = 1.5 terrestrial spectrum shown in Figure 8.

The solar spectral distribution shown in Figure 7 for m = 0 is the World Radiation Center's 1985 standard extraterrestrial spectrum for a solar constant of 1367 Wm^2 (Wehrli 1985). The one for m = 1.5 in Figure 8 is from ASTM *Standard* E 891. This latter takes no account of monthly variations in irradiance caused by changes in the

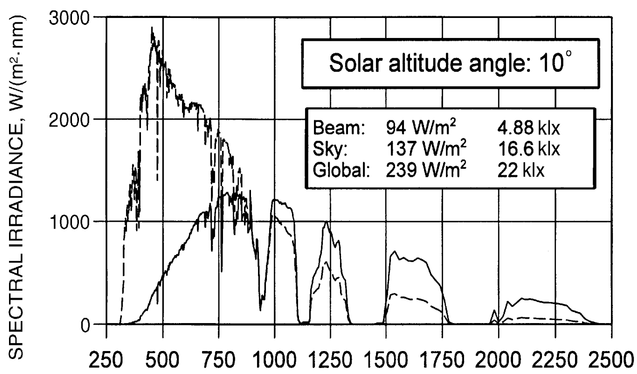

Fig. 9 Comparison of Direct and Diffuse Solar Spectra for Low Solar Altitude Angle

earth-sun distance and by variations in the atmosphere's constituent particulates and gases.

When variations in atmospheric constituents and air mass are considered, the solar spectral distribution is seen to vary, as illustrated in Figure 8, for two different atmospheric conditions and for two solar altitude angles, and in Figure 9 for both direct and diffuse radiation components and a low sun angle. It is clear that the spectral distribution for low sun angle beam radiation is significantly shifted toward longer wavelengths. This shift can be seen visually as a reddening of the sun near to the horizon. Clear sky diffuse radiation is generally shifted toward the blue end of the spectrum.

Upon passage through the atmosphere, extraterrestrial solar radiation is reduced in magnitude due to absorption by atmospheric gases and particulates. The strength of this absorption varies with wavelength, and the terrestrial solar spectrum exhibits definite "dips" in regions of strong absorption, called **absorption bands**. The most prominent atmospheric gases contributing to this effect are listed below:

- **Ozone.** Strongest absorption in the ultraviolet, some in the visible. Concentration variable.
- **H_2O.** Strongest absorption in near and far IR. Highly variable.
- **CO_2.** Strongest absorption in near and far IR. Slightly variable.
- **O_2, CH_4, N_2O, CFCs.** Strongest absorption mostly in the IR. Concentration almost constant.
- **NO_2.** Strongest absorption in the visible. Highly variable in polluted areas.

The effect of aerosols and other particulates on terrestrial solar radiation can be significant. Diffuse sky radiation is solar beam radiation that has been multiply scattered out of the direct beam and downward through the atmosphere to the earth's surface. This scattering is produced by 30 different atmospheric molecules (of which the above are the most significant optically) and by larger particles of different types, including aerosols of water, dust, smoke, and particulates of other kinds.

More information on atmospheric optics can be found in Chapter 44 of the Optical Society of America's *Handbook of Optics* (Bass 1995) and in Iqbal (1983).

Glazing systems exhibiting strong spectral selectivity (strong changes in their optical properties over the solar spectrum) will selectively pass more or less radiation in different parts of the spectrum. This effect can cause substantial changes in the solar heat gain coefficient of the glazing system when the shape of the solar spectrum shifts appreciably. This in turn can cause errors in solar heat gain predictions when the actual solar radiation on a fenestration system has a spectrum that is different from the standard spectrum used to determine the solar heat gain coefficient of that system (McCluney 1996). These errors are typically 5 to 10% but can be substantially greater in special cases.

Some short-wavelength radiation scattered by air molecules, dust, and other particulates in the atmosphere reaches the earth in the form of diffuse sky radiation E_d. Since this diffuse radiation comes from all parts of the sky, its irradiance is difficult to predict and varies as moisture and particulate content and sun angle change throughout any given day. For completely overcast conditions, the diffuse component accounts for all solar radiant heat gain of fenestrations.

The total short-wavelength irradiance E_t reaching a terrestrial surface is the sum of the direct solar radiation E_D, the diffuse sky radiation E_d, and the solar radiation E_r reflected from surrounding surfaces. The irradiance on the fenestration aperture of the direct beam component E_D is the product of the direct normal irradiation E_{DN} and the cosine of the angle of incidence θ between the incoming solar rays and a line normal (perpendicular) to the surface:

$$E_t = E_{DN}\cos\theta + E_d + E_r \tag{12}$$

A method for computing all the factors on the right side of Equation (12) is presented in the sections on Direct Normal Irradiance and Diffuse and Ground-Reflected Radiation. Perez et al. (1986), Gueymard (1987), *Solar Energy* (1988), and Gueymard (1993) give more detailed models, which separate the diffuse sky radiation into different components. Gueymard (1995) provides a comprehensive spectrally based model for calculating the spectral and broadband totals of all three terms in Equation (12), for cloudless sky conditions. The Gueymard model allows user input of the concentrations of a variety of atmospheric constituents, including particulates.

The importance of the diffuse component is illustrated in Figure 9, which shows that at low sun angles the diffuse component contains more radiant flux than the direct beam component, even on a clear day, and that the spectral distributions of the two components are quite different. Although the total irradiances are relatively modest for both of these components, they are not insignificant for annual energy performance calculations.

Vertical windows receive considerable quantities of diffuse sky radiation over the course of a year. The diffuse component is an important part of solar radiant heat gain.

Determining Solar Angle

The sun's position in the sky is conveniently expressed in terms of the solar altitude β above the horizontal and the solar azimuth φ measured from the south (Figure 10). These angles, in turn, depend on the local latitude L; the solar declination δ, which is a function of the date [Table 7 or Equation (11)]; and the apparent solar time, expressed as the hour angle H, where

$$H = 15(\mathrm{AST} - 12) \tag{13}$$

Equations (14) and (15) relate β and φ to the three angles just mentioned:

$$\sin\beta = \cos L\cos\delta\cos H + \sin L\sin\delta \tag{14}$$

$$\cos\phi = \frac{\sin\beta\sin L - \sin\delta}{\cos\beta\cos L} \tag{15}$$

Figure 10 shows the solar position angles and incident angles for horizontal and vertical surfaces. Line OQ leads to the sun, the north-south line is NOS, and the east-west line is EOW. Line OV is perpendicular to the horizontal plane in which the solar azimuth φ (angle HOS) and the surface azimuth Ψ (angle POS) are located. Angle HOP is the surface solar azimuth γ, defined as

$$\gamma = \phi - \psi \tag{16}$$

The solar azimuth φ is positive for afternoon hours and negative for morning hours. Likewise, surfaces that face west have a positive

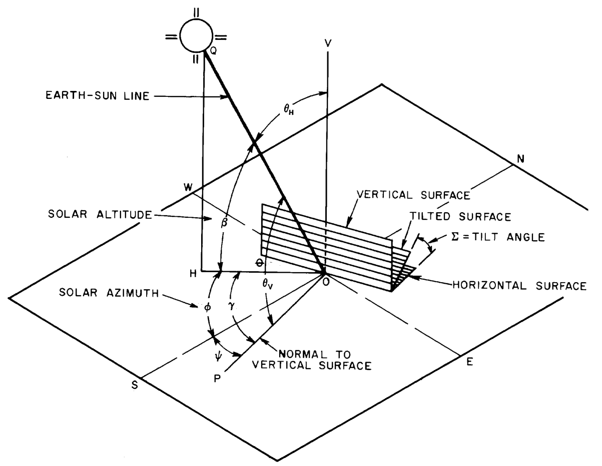

Fig. 10 Solar Angles for Vertical and Horizontal Surfaces

Table 9 Surface Orientations and Azimuths, Measured from South

Orientation	N	NE	E	SE	S	SW	W	NW
Surface azimuth ψ	180°	−135°	−90°	−45°	0	45°	90°	135°

surface azimuth ψ; those facing east have a negative surface azimuth (Table 9). If γ is greater than 90°or less than −90°, the surface is in the shade. Table 9 gives values in degrees for the surface azimuth ψ, applicable to the orientations of interest.

The angle of incidence θ for any surface is defined as the angle between the incoming solar rays and a line normal to that surface. For the horizontal surface shown in Figure 10, the incident angle θ_H is QOV; for the vertical surface, the incident angle θ_V is QOP.

For any surface, the incident angle θ is related to β, γ, and the tilt angle of the surface Σ by

$$\cos\theta = \cos\beta\cos\gamma\sin\Sigma + \sin\beta\cos\Sigma \qquad (17)$$

where Σ = tilt angle of surface from horizontal.

When the surface is horizontal, $\Sigma = 0°$ and

$$\cos\theta_H = \sin\beta \qquad (18)$$

For a vertical surface, $\Sigma = 90°$ and

$$\cos\theta_V = \cos\beta\cos\gamma \qquad (19)$$

Direct Normal Irradiance

At the earth's surface on a clear day, direct normal irradiation, or solar irradiance E_{DN}, is represented by

$$E_{DN} = \frac{A}{\exp(B/\sin\beta)} \qquad (20)$$

where

A = apparent solar irradiation at air mass $m = 0$ (Table 7)
B = atmospheric extinction coefficient (Table 7)

Values of A and B vary during the year because of seasonal changes in the dust and water vapor content of the atmosphere and because of the changing earth-sun distance. Equation (20) does not give the maximum value of E_{DN} that can occur in each month but yields values that are representative of conditions on cloudless days for a relatively dry and clear atmosphere. For very clear atmospheres, E_{DN} can be 15% higher than indicated by Equation (20), using values of A and B in Table 7.

For locations where clear, dry skies predominate (e.g., at high elevations) or, conversely, where hazy and humid conditions are frequent, values found by using Equation (20) and Table 7 should be

Table 10 Solar Reflectances of Foreground Surfaces

	Incident Angle					
Foreground Surface	**20°**	**30°**	**40°**	**50°**	**60°**	**70°**
New concrete	0.31	0.31	0.32	0.32	0.33	0.34
Old concrete	0.22	0.22	0.22	0.23	0.23	0.25
Bright green grass	0.21	0.22	0.23	0.25	0.28	0.31
Crushed rock	0.20	0.20	0.20	0.20	0.20	0.20
Bitumen and gravel roof	0.14	014	0.14	0.14	0.14	0.14
Bituminous parking lot	0.09	0.09	0.10	0.10	0.11	0.12

Adapted from Threlkeld (1962)

multiplied by the Clearness Numbers in Threlkeld and Jordan (1958), reproduced as Figure 5 in Chapter 32 of the 1999 *ASHRAE Handbook—Applications*. This broadband model should only be used for determining fenestration solar gain when the glazing system is not strongly spectrally selective and when its angular selectivity closely matches that of single-pane glass.

Diffuse and Ground-Reflected Radiation

The following equations can be used to generate E_d and E_r, where all angles are in degrees. The solar azimuth ϕ and the surface azimuth ψ are measured in degrees from south; angles to the east of south are negative, and angles to the west of south are positive. Values of *A, B,* and *C* are given in Table 7 for the 21st day of each month. Values for other dates can be obtained by interpolation.

The ratio Y of sky diffuse radiation on a vertical surface to sky diffuse radiation on a horizontal surface is given by

$$\begin{aligned} Y &= 0.55 + 0.437\cos\theta + 0.313\cos^2\theta && \text{for } \cos\theta > -0.2 \\ Y &= 0.45 && \text{for } \cos\theta \le -0.2 \end{aligned} \qquad (21)$$

Diffuse irradiance E_d is given by

$$E_d = CYE_{DN} \qquad \text{for vertical surfaces} \qquad (22)$$

$$E_d = CE_{DN}\frac{1 + \cos\Sigma}{2} \qquad \text{for surfaces other than vertical} \qquad (23)$$

Ground-reflected irradiance E_r is given by

$$E_r = E_{DN}(C + \sin\beta)\rho_g\frac{1 - \cos\Sigma}{2} \qquad \text{for surfaces at all orientations} \qquad (24)$$

where ρ_g is ground reflectivity, often taken to be 0.2 for typical mixture of ground surfaces. For other surfaces, Table 10 lists angle-dependent solar reflectances.

Example 5. Find the solar azimuth and altitude at 3:00 P.M. central daylight savings time on June 21 in St. Louis, MO.

Solution: Central daylight savings time of 3:00 P.M. re-expressed in decimal hours at local standard time is LST = 14.0. The latitude and longitude of St. Louis, MO, are 38.6°N and 90.2°W, respectively. The local standard meridian of the central time zone is 90°W. The equation of time (Table 7) is −1.4 min. From Equation (10), apparent solar time (AST) = 14.0 − 1.4/60 + (90 − 90.2)/15 = 13.9633. From Equation (13), $H = 15 \times (13.9633 - 12) = 29.45°$. Table 7 gives the solar declination δ on June 21 as 23.45°.

Thus, by Equation (14),

$$\sin\beta = \cos(38.6°)\cos(23.45°)\cos(29.45°) + \sin(38.6°)\sin(23.45°) = 0.873$$
$$\beta = 60.76°$$

Using Equation (15),

$$\cos\phi = \frac{\sin(60.76)\sin(38.6) - \sin(23.45)}{\cos(60.76)\cos(38.6)} = 0.384$$

$$\phi = 67.4°$$

Example 6. For the conditions of Example 5, find the incident angle at a window facing west.

Solution: From Example 5, ϕ = 67.4°. From Table 9, ψ = 90°. From Equation (16), γ = 67.4° – 90° = –22.6°.

A negative surface solar azimuth γ indicates that the sun is south of the normal to the surface. Thus, using Equation (19),

$\cos\theta = \cos(60.76°)\cos(-22.6°) = 0.451$
$\theta = 63.2°$

Example 7. Find the direct, diffuse, and ground-reflected components of the solar irradiation on the window in Example 6.

Solution: From Example 5, sin β = 0.873, and from Table 7, A = 1088 W/m^2 and B = 0.205. Therefore, from Equation (20),

$$E_{DN} = 1088/[\exp(0.205/0.873)] = 860.3 \text{ W/m}^2$$

$$E_{DN}\cos(\theta) = 860.3 \times 0.451 = 388 \text{ W/m}^2$$

From Table 7, C = 0.134. From Equation (21), $Y = 0.55 + 0.437 \times 0.451 + 0.313 \times (0.451)^2 = 0.811$. From Equation (22),

$$E_d = (0.134)(0.811)(860.3) = 93.5 \text{ W/m}^2$$

From Equation (24), assuming a ground reflectivity ρ_g of 0.2,

$$E_r = (860.3)(0.134 + 0.873)(0.2)/2 = 86.6 \text{ W/m}^2$$

Thermal Infrared Radiation

Any material above a temperature of absolute zero emits electromagnetic radiation. The rate of emission depends upon the temperature of the material and can be expressed in a simple equation, called the Stefan-Boltzmann law:

$$E_b = \sigma T^4 \qquad (25)$$

where

E_b = hemispherical total emissive power of black body, W/m^2
T = temperature, K
σ = Stefan-Boltzmann constant, W/(m$^2\cdot$K^4)

The **emissivity** e of a surface is the ratio of the emission of thermal radiant flux from the surface to the flux that would be emitted by a blackbody emitter at the same temperature. Given the temperature and emissivity of a surface, the emitted irradiance spectrum can be computed from

$$E = e\sigma T^4$$

where E is the emitted irradiance in units of flux per unit area, e is the emissivity of the surface, σ is the Stefan-Boltzmann constant, and T is the absolute temperature of the surface.

The maximum value of **hemispherical emissivity** e for any material is 1.0, in which case the surface emits the theoretical maximum amount of radiation possible. In this case, the surface is called a **blackbody**, and the radiation emitted by the surface is called **blackbody radiation**.

Occasionally, a related quantity called **normal emissivity** is used. The relationship between them is illustrated in Figure 11. The spectral distribution of blackbody radiation is illustrated in Figure 12 for temperatures ranging from 300 K (room temperature) to 20 000 K.

OPTICAL PROPERTIES

Solar radiation (including both direct rays from the sun and diffuse rays from the sky, clouds, and surrounding objects) incident on a fenestration system is partly transmitted and partly reflected by the glazings of that system. An additional fraction is absorbed within the glazings and/or the coatings on their surfaces. The fraction of incident flux that is reflected is called the **reflectance** R, the fraction absorbed is called the **absorptance** $\mathcal{A}$, and the fraction transmitted is the **transmittance** T. The sum of the transmittance T, absorptance $\mathcal{A}$, and reflectance R of a glazing layer is unity:

$$T + R + \mathcal{A} = 1 \qquad (26)$$

However, this is complicated by the fact that radiation incident on a surface can have nonconstant distributions over the directions of incidence and over the wavelength (or frequency) scale. Thus, when measuring one or more of the optical properties, the wavelength distribution and direction of incident (and emerging) radiation must be specified.

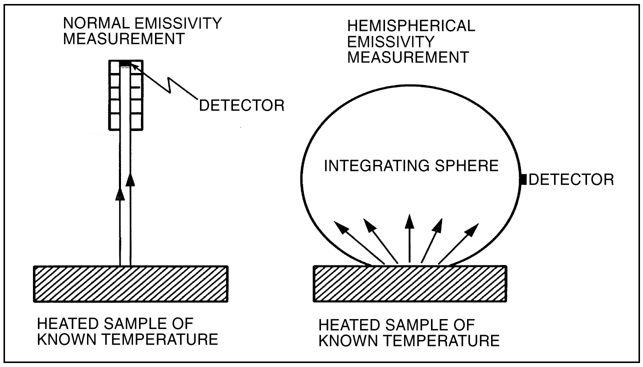

Fig. 11 Illustration of Difference Between Normal and Hemispherical Emissivity

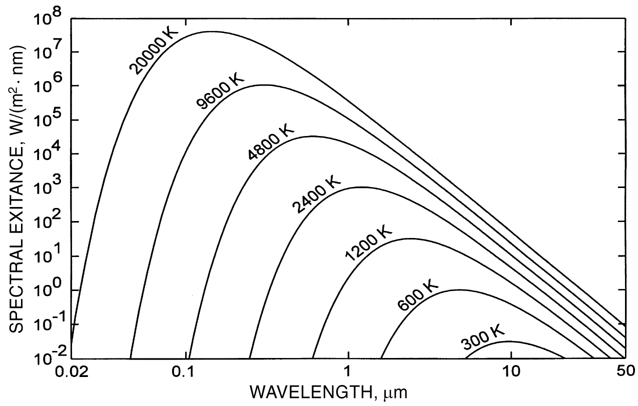

Fig. 12 Spectral Distributions of Blackbody Radiation at Different Source Temperatures

Angular Dependence

The concept of solid angle is needed to understand angular dependence. A solid angle is defined and enclosed by all rays joining a point to a closed curve. For a closed curve on a sphere of radius R, the solid angle ϖ is the ratio of the projected area A on the sphere to the square of R. A sphere has a solid angle of 4π steradians (4π sr); a hemisphere has a 2π sr solid angle.

Radiation incident on a point in a surface comes to that point from many directions in some solid angle. For a cone of half angle α, the solid angle defined by the circular top and point bottom of that cone is given by

$$\varpi = 2\pi(1 - \cos\alpha) \qquad (27)$$